Magnetic and magnetocaloric properties of Sm1xCaxMnO3 (x = 0.88) nanoparticles

by Kontan Tarigan

Submission date: 07-Apr-2019 02:53PM (UTC+0700)
Submission ID: 1107319046
File name: 2017-JMMM.pdf (703.04K)
Word count: 5345
Character count: 23717

Journal of Magnetism and Magnetic Materials 443 (2017) 233–238

Contents lists available at ScienceDirect

Journal of Magnetism and Magnetic Materials

journal homepage: www.elsevier.com/locate/jmmm

Research articles

Magnetic and magnetocaloric properties of $Sm_{1-x}Ca_xMnO_3$ ($x = 0.88$) nanoparticles

T.L. Phan [a,*], N.T. Dang [b], T.A. Ho [c], J.S. Rhyee [d], W.H. Shon [d], K. Tarigan [e], T.V. Manh [f]

[a] Department of Physics and Oxide Research Center, Hankuk University of Foreign Studies, Yongin 449-791, South Korea
[b] Institute of Research and Development, Duy Tan University, Da Nang, Viet Nam
[c] Department of Materials Science and Engineering, Korea University, Seoul 136-713, South Korea
[d] Department of Applied Physics & KHU-KIST Department of Converging Science and Technology, Kyung Hee University, Yongin 17104, South Korea
[e] Department of Mechanical Engineering, Mercu Buana University, Jakarta-Barat, Jakarta 11650, Indonesia
[f] Advanced Institute for Science and Technology, Hanoi University of Science and Technology, Dai Co Viet, Hai Ba Trung, Hanoi, Viet Nam

ARTICLE INFO

Article history:
Received 28 March 2017
Accepted 20 July 2017
Available online 20 July 2017

Keywords:
Perovskite manganites
Nanoparticles
Magnetocaloric effect

ABSTRACT

We used the mechanical milling to prepare orthorhombic $Sm_{0.12}Ca_{0.88}MnO_3$ samples with the average crystallite size (d) changing from 100 to 139 nm. Their magnetic and magnetocaloric properties were then studied upon magnetization data versus the temperature and magnetic field, $M(T, H)$. The results revealed the samples undergoing the ferromagnetic-paramagnetic (FM-PM) phase transition at the Curie temperature $T_C \approx 110$ K. Around this transition, the magnetic-entropy change (ΔS_m) reaches the maxima. The maximum $|\Delta S_m|$ values are about 2–4 $J \cdot kg^{-1} \cdot K^{-1}$, corresponding to relative cooling power of 35–60 $J \cdot kg^{-1}$, for an applied field $H = 30$ kOe. The assessments based on Banerjee's criteria and constructing a universal curve for $|\Delta S_m(T, H)|$ data indicate the samples having the nature of a second-order phase transition. Also, the detailed analyses based on the Curie-Weiss law and magnetic-order exponent prove the existence of the Griffiths phase and magnetic inhomogeneity in the samples. These properties would be changed by changing d.

1. Introduction

Orthorhombic $SmMnO_3$ is an insolating A-type antiferromagnetic (AFM) compound with the Néel temperature $T_N \approx 60$ K. Mn^{3+} moments are aligned ferromagnetically within the ab plane, but antiferromagnetically in the c direction. It means that its A-type AFM structure has spin canting along the c axis [1]. The origin of the canting has been discussed in terms of the single-ion anisotropy and Dzyaloshinskii-Moriya interactions [2,3]. Comparing with other manganite compounds, $SmMnO_3$ shows some noticeable properties, such as magnetocapacitive effects and temperature-induced magnetization reversal/negative magnetization opposite to the magnetic-field direction [1]. The two latter phenomena are ascribed to the canted Mn^{3+} moments whose direction is the opposite of the polarized Sm^{3+} moments, which are usually observed in Néel's N-type ferrimagnetic compounds with two or more magnetic sublattices [1,2].

However, with the doping of an alkaline-earth element into the Sm^{3+} site, such as $Sm_{1-x}(Ca, Sr)_xMnO_3$ compounds, the canting is gradually declined due to the additional presence of Mn^{4+} ions. This stimulates ferromagnetic (FM) and AFM interactions associated with Mn^{3+}-Mn^{4+}, and Mn^{4+}-Mn^{4+} and/or $Mn^{3+,4+}$-Sm^{3+} pairs, respectively (besides pre-existing Mn^{3+}-Mn^{3+} and/or Mn^{3+}-Sm^{3+} pairs in $SmMnO_3$) [4], and the crystal-structure changes (for example, the orthorhombic-monoclinic transition [5,6]). By varying doping content (x) in $Sm_{1-x}(Ca, Sr)_xMnO_3$, their electrical, magnetic and magnetotransport properties can be enriched as expected [2,6–9]. It is worth noting that because both Mn and Sm ions contribute magnetic interactions, much more intriguing and complex properties have been found in these compounds, including the A-, C-, G-, CE-type AFM, FM, paramagnetic (PM), spin/cluster glass, charge ordering, orbital ordering, Griffiths phase, and so forth [5,6,8–10]. Particularly, with suitable x content, it could be found colossal magnetoresistance (MR) and magnetocaloric (MC) effects [5,11,12]. Such phenomena are generated from strong interplay between spin, charge, orbital and lattice degrees of freedom. Together with double-exchange (DE) mechanism proposed for Mn^{3+}-Mn^{4+} FM exchange pairs [13], Jahn-Teller distortions caused by strong spin-lattice coupling have been also involved to explain effectively the colossal CMR and MC effects [14,15].

* Corresponding author.
E-mail address: ptlong2512@yahoo.com (T.L. Phan).

http://dx.doi.org/10.1016/j.jmmm.2017.07.064
0304-8853/

Concerning a magnetic phase diagram of $Sm_{1-x}Ca_xMnO_3$, it has been found that the FM phase is dominant as $0 < x \leq 0.4$, the *CE*- and/or *C*-type AFM phases exist as $0.4 < x < 0.8$, and the *G*-type AFM and/or FM phase appear as $x > 0.9$ [6,8]. Interestingly, in the range of $x = 0.8–0.9$, besides the *C*- and *G*-type AFM + FM phases [6] and their transition around $x \approx 0.85$, there is the Griffiths phase found for $x > 0.85$ [5,6,10]. One can improve outstanding properties of this material system upon the Ru doping [16]. Though their electrical, transport and magnetic properties were investigated carefully, the MC effect, FM-PM phase-transition nature, and the crystallite-size influence on the magnetic property of these material types have not been taken into account in detail yet [5,6,10,16,17]. Dealing with these problems, we have selected a typical composition of $Sm_{0.12}Ca_{0.88}MnO_3$ showing simultaneously the FM and Griffiths phases, with $T_N(G) \approx T_C$ [5,10] and highest magnetic moment [17], and then studied the influence of the crystallite size (d) on its magnetic and MC properties. We point out that the d change from 100 to 139 nm does not change the T_C, and the nature of its second-order phase transition (SOPT). Besides the persistence of the Griffiths phase, we also found an increase of magnetic disorder with decreasing d. This factor causes the gradual reduction of the magnetization (M) and MC effect.

2. Experimental details

Three $Sm_{0.12}Ca_{0.88}MnO_3$ samples with different d values were prepared by solid-state reaction in air combined with high-energy ball milling. First, a polycrystalline sample was synthesized from high-purity powders (99.9%) of La_2O_3, CaO, $MnCO_3$, and Sm_2O_3. These powders were combined in nominal quantities of $Sm_{0.12}Ca_{0.88}MnO_3$, and well mixed by using an agate mortar and pestle. The mixture was then pre-annealed at 1200 °C for 48 h. After pre-annealing, the mixture was ground and pressed into a pellet and annealed at 1300 °C for 48 h. The final pellet was divided into small parts. Two parts were in turn ground for different times (t_m) of 10 and 20 min (min) by using a mechanical milling machine; the as-prepared sample is indicated as t_m=0 min. To minimize undesired impurities generated during the milling process, we used a nonmagnetic grinding medium consisting of a zirconia vial (45 mL volume) and two balls (~13 mm diameter) purchased from SPEX-SamplePrep. A ball-to-powder mass ratio of 5.5 was fixed for each sample. The crystal structure of the final products were checked by using an X-ray diffractometer (Bruker AXS, D8 Discover) working with a Cu-Kα_1 radiation source (λ = 1.5406 Å). Before taking X-ray diffraction (XRD) patterns, a small Si amount was mixed with the powder samples to limit errors caused by the position calibration of an X-ray incident beam. Magnetization measurements were carried out on a physical property measurement system (PPMS, Quantum Design), where the temperature and magnetic field were tuned in the ranges $T = 5–300$ K and $H = 0–30$ kOe, respectively.

3. Results and discussion

Fig. 1(a) shows powder XRD patterns of fabricated $Sm_{0.12}Ca_{0.88}MnO_3$ samples. Our analyses demonstrate the single-phase samples crystallized in the *Pnma* orthorhombic structure, corresponding to the Miller-indexed peaks. With increasing t_m, the diffraction peaks shift slightly (about 0.02°) towards smaller angles. Concurrently, the enhanced linewidth (β) and reduced intensity of the peaks are also found, as shown in Fig. 1(b) for the (0 0 2) peak. This is related to the d reduction, and the increase of lattice strain and defects [18]. Using the Scherrer equation $d = k\lambda/\beta\cos\theta$, with the shape factor $k \approx 0.9$, we calculated average d values to be about 139, 122, and 100 nm for the samples with

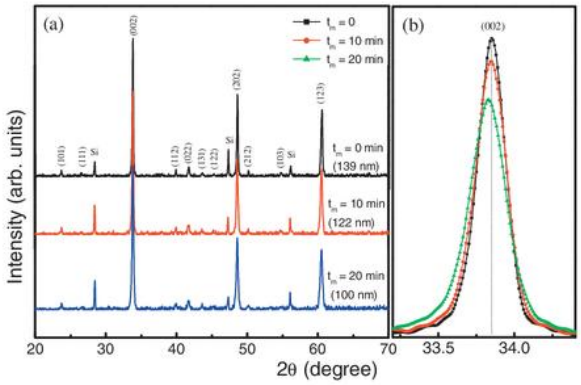

Fig. 1. (a) Room-temperature XRD patterns, and (b) an enlarged view of the (0 0 2) peak of the $Sm_{0.12}Ca_{0.88}MnO_3$ samples with t_m = 0, 10 and 20 min.

t_m = 0, 10, and 20 min, respectively, as shown in Table 1 and Fig. 1(a). Hereafter, we use the values of d instead of t_{min} as talking about the samples. Having carried out Rietveld refinements for the XRD patterns, we also obtained the lattice constants (a, b, c) and unit-cell volume (V). As listed in Table 1, the values a = 5.293 Å, b = 5.295 Å, c = 7.481 Å and V = 209.66 Å^3 obtained for the as-prepared sample (d = 139 nm) are in good agreement with those reported by Kim et al. [5] on $Sm_{1-x}Ca_xMnO_3$ with $x = 0.8–0.92$. These parameters tend to decrease with decreasing d, which could be due to the loss of oxygen ions, and lattice distortions caused by the milling process.

To study the influence of the d reduction on the magnetic property, we first measured temperature-dependent magnetization, $M(T)$, for an applied field H = 100 Oe. Fig. 2(a) shows $M(T)$ data recorded under the zero-field-cooled condition, with $T = 10–150$ K. M of all the samples gradually increases with increasing T from 10 to–100 K, and reaches the maxima at ~105 K. These phenomena are relatively popular in perovskite manganites, and ascribed to the existence of FM clusters, magnetic inhomogeneity, and/or glassy state [10,19,20]. If increasing T above ~105 K, M decreases quickly to zero, as a result of the FM-PM phase transition. It is worth noting that the feature of the $M(T)$ curves indicates the absence of the *G*-type AFM phase. This is due to the dominancy of Mn^{3+}-Mn^{4+} FM interactions in $Sm_{0.12}Ca_{0.88}MnO_3$, resulting in $T_N(G) \approx T_C$ [10]. By plotting the dM/dT versus T curves, Fig. 2(b), we determined the T_C values (≈110 K) from their minimum point. It appears that the d change from 100 to 139 nm almost does not change the T_C. However, if more attention is given to the inverse susceptibility, $\chi^{-1}(T) = H/M(T)$, Fig. 2(c), one can see the $\chi^{-1}(T)$ magnitudes of the samples in the PM region ($T > 110$ K) are different and dependent on d. All the $\chi^{-1}(T)$ curves exhibit the Griffiths phase (GP) like downturn below a certain temperature, the so-called Griffiths temperature (T_G), where there is the deviation of the inverse susceptibility from the Curie–Weiss (C-W) law. This phenomenon was also found in bulk $Sm_{1-x}Ca_xMnO_3$ samples with $x = 0.85–0.92$ [5,10]. As listed in Table 1, T_G values are 126 K for d = 122 and 139 nm, and 131 K for d = 100 nm. In the temperature range $T_C < T < T_G$, there is a large correlated FM clusters within the globally PM phase, leading to the temperature-dependent susceptibility that can be described by a power function $\chi^{-1} \propto (T - T_C^{rand})^{1-\lambda}$, where T_C^{rand} is the random transition temperature lying between T_C and T_G, and λ (with $0 \leq \lambda < 1$) is a non-universal positive exponent [21]. The T_G increase demonstrates more stimulated magnetic inhomogeneity when d reduces, similar to the cases of $Sm_{0.5}Sr_{0.5}MnO_3$ [22] and $La_{0.67}Sr_{0.33}MnO_3$ [23]. Particularly, at temperatures $T > T_G$, the PM behavior of

Table 1
Experimental values obtained for $Sm_{0.12}Ca_{0.88}MnO_3$ samples with various crystallite sizes d = 100–139 nm.

t_m	d	a	b	c	V	T_C	T_G	θ	P_{eff}
(min)	(nm)	(Å)	(Å)	(Å)	(Å^3)	(K)	(K)	(K)	(μ_B)
0	139	5.293	5.295	7.481	209.66	110	126	95	3.53
10	122	5.290	5.301	7.475	209.59	110	126	101	3.42
20	100	5.271	5.273	7.458	207.29	110	131	104	3.33

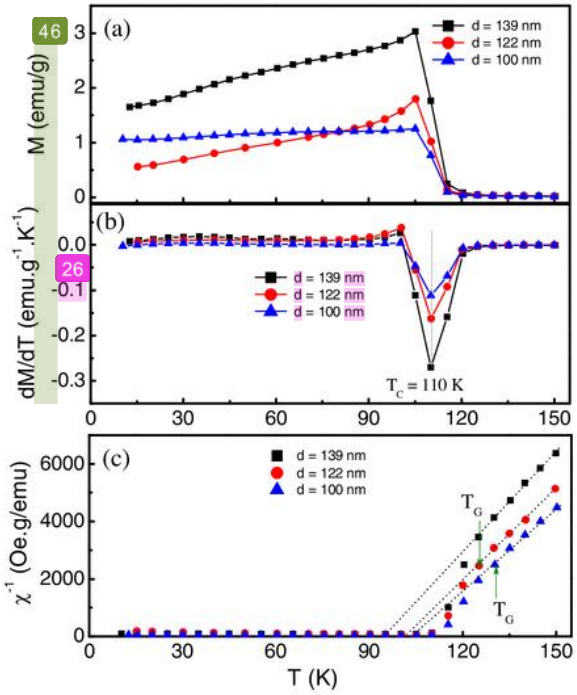

Fig. 2. Temperature dependences of (a) M, (b) dM/dT, and (c) χ^{-1} for $Sm_{0.12}Ca_{0.88}MnO_3$ samples with various d values in the field H = 100 Oe, where temperature-increment steps were fixed at 5 K.

$\chi^{-1}(T)$ can be described well by the C-W law $\chi(T) = C/(T-\theta)$, where C and θ are the Curie constant and C-W temperature, respectively, obtained from fitting the $\chi^{-1}(T)$ data at temperatures $T > T_G$. Using the relation $C = N(\mu_B P_{eff})^2/3k_B$, where $N = 6.023 \times 10^{23}$ mol^{-1} is the number of ions, k_B=1.3806 × 10^{-23} J/K is the Bolzmann constant, and μ_B = 9.274 × 10^{-24} J/T is the Bohr magneton, we would calculate the effective PM moment (P_{eff}) values to be 3.55μ_B, 3.42μ_B, and 3.33μ_B for the samples with d = 139, 122, and 100 nm, respectively. These P_{eff} and θ values are listed in Table 1. In theory, in the PM region without the orbital moment contribution, the spin moments of Mn^{3+} (P_{eff} = 4.9μ_B), Mn^{4+} (P_{eff} = 3.9μ_B) and Sm^{3+} (P_{eff} = 5.5μ_B) ions all contribute to the PM susceptibility of $Sm_{0.12}Ca_{0.88}MnO_3$, resulting in its theoretical P_{eff} value of ~4.61μ_B. Clearly, the experimental P_{eff} values are smaller than the theoretical value. This could be due to spin-orbital coupling and/or disorder spins between magnetic moments existing in the $Sm_{0.12}Ca_{0.88}MnO_3$ samples. Previously, it has been found that the d decrease to the nanoscale leads to the formation of magnetically dead (spin-glass-like) surface layers. Their existence reduces the FM correlation length and magnetization as well [23–26].

Such decreased magnetic order and enhanced magnetic inhomogeneity when d reduces would influence directly the MC effect and FM-PM transition nature. To further understand these problems, we recorded field-dependent magnetization at different temperatures, $M(T, H)$, around the FM-PM transition. Fig. 3(a, b) show $M(T, H)$ data of typical samples with d = 139 and 100 nm. At a specific temperature T, the d decrease causes a gradual reduction of M. Concurrently, M increases with increasing H due to the alignment of magnetic moments to the field direction. In the FM region, $M(H)$ curves are nonlinear, which become linear in the PM region. A temperature increase from the FM region to the PM one reduces gradually M. Particularly, a large gap between $M(H)$ curves are found around the FM-PM transition, where FM coupling is strongly declined by thermal energy. This phase transition can be seen more clearly if performing H/M versus M^2 plots, as shown in Fig. 3(c, d). At low fields, the H/M-M^2 curves are driven to two opposite directions, which are characteristic of the FM and PM regions [27]. Particularly, their curvature is decreased quickly when T approaches close to the T_C. At all temperatures the slopes of the H/M-M^2 curves are positive. This proves all the samples undergoing a second-order phase transition (SOPT), according to Banerjee's criteria [28]. If carefully considering the feature of the H/M-M^2 curves at temperatures $T \approx T_C$, Fig. 3(c, d), one can see that H/M-M^2 dependences are relatively linear for the d = 139 nm sample (and d = 122 nm as well, not shown) and nonlinear for the d = 100 nm sample. This is ascribed to long-range FM order in the d = 122 and 139 nm samples, and short-range FM order in the d = 100 nm sample [27,29]. Based on the mean-field theory, Skomski showed that long-range FM interactions could be established in complex spin structures with two or more sub-lattices [30]. It is known that small changes in the crystal structure, concentration of magnetic atoms/ions, and chemical pressure can change remarkably FM order. For the case of the as-prepared $Sm_{0.12}Ca_{0.88}MnO_3$ sample (d = 139 nm) with the mixed valence of $Mn^{3+,4+}$ and Sm^{3+} ions, the FM interaction associated with Mn^{3+}-Mn^{4+} exchange pairs is strongest, resulting in $T_N(G) \approx T_C$ [5,10]. Meanwhile, AFM couplings between Sm^{3+}, Mn^{3+} and/or Mn^{4+}, if possible, are weak. Long-range FM order is thus ascribed to the Mn^{3+}-Mn^{4+} FM double-exchange pairs. When d

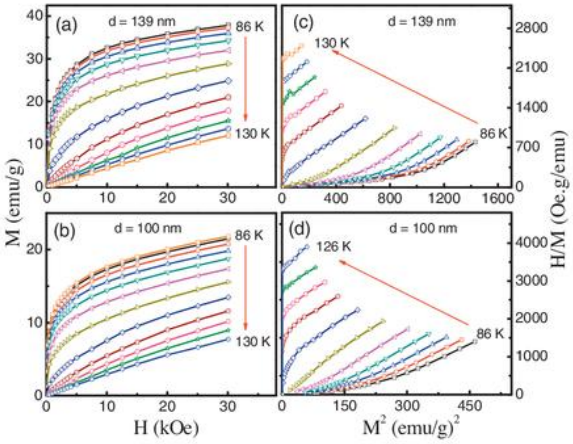

Fig. 3. $M(H)$, and H/M versus M^2 curves for typical $Sm_{0.12}Ca_{0.88}MnO_3$ samples with (a, c) d = 139 nm and (b, d) d = 100 nm around their FM-PM phase transition, with temperature increments of 4 K.

decreases to 100 nm, there is the formation of magnetically dead surface layers. It means that the AFM interactions increase with decreasing d. Short-range FM order is thus established as a consequence of strong interaction between the FM and AFM phases.

From the $M(H, T)$ data, Fig. 3(a, b), we can assess the MC effect of the samples based on the magnetic-entropy change (ΔS_m). For a ferromagnet undergoing a SOPT, the calculation of $\Delta S_m(T, H)$ can be based on Maxwell's relations [31]

$$\left(\frac{\partial S_m}{\partial H}\right)_T = \left(\frac{\partial M}{\partial T}\right)_H, \quad (1)$$

$$\Delta S_m(T,H) = S_m(T,H) - S_m(T,0) = \int_0^H \left(\frac{\partial M}{\partial T}\right)_H dH, \quad (2)$$

where the magnetic-field interval varies from 0 to H. Fig. 4 shows the $|\Delta S_m(T, H)|$ data of the samples with d = 100, 122, and 139 nm. In the studying T range, $|\Delta S_m|$ increases with increasing H from 0 to 30 kOe. It reaches the maxima (denoted by $|\Delta S_{max}|$) around the FM-PM transition, where the order-to-disorder transformation of magnetic moments takes place strongly. Decreasing d from 139 to 100 nm reduces quickly the values of $|\Delta S_m|$ as well as $|\Delta S_{max}|$. In our work, field dependences of $|\Delta S_{max}|$, with H = 0–30 kOe, can be described by a power function [32]

$$|\Delta S_{max}| \alpha H^n, \quad (3)$$

where n is a local order-magnetic parameter, with n = 0.65, 0.70, and 0.72 for the d = 139, 122 and 100 nm samples, respectively, as shown in Fig. 5(a). For a ferromagnet with long-range FM interactions, n is equal to ~0.67 [32]. A large deviation of n from the theoretical value (~0.67) determined for the d = 100 nm sample demonstrates the absence of long-range FM order. Particularly, under an applied field span of H = 30 kOe, we obtained the $|\Delta S_{max}|$ values for d = 139, 122, and 100 nm to be about 4.2, 2.6, and 2.0 J·kg^{-1}·K^{-1}, respectively. These values are smaller than those recorded for $Sm_{0.58}Sr_{0.42}MnO_3$ with d = 96–280 nm ($|\Delta S_{max}|$ = 5 ~ 9 J·kg^{-1}·K^{-1} for H = 30 kOe) [25]) and $La_{0.7}Ca_{0.3}MnO_3$ with d = 72–200 nm ($|\Delta S_{max}|$ = 4 ~ 9 J·kg^{-1}·K^{-1} for H = 30 kOe) [33] having the first-order nature. However, for magnetic compounds with the second-order nature, such as $La_{0.7}Ca_{0.3}MnO_3$ with d = 45–54 nm [33] and $La_{0.7}Ca_{0.3-x}Ba_xMnO_3$ (x = 0.025, and 0.05) with $d \approx 40$ nm [34], their $|\Delta S_{max}|$ values (2.2 ~ 4.4 J·kg^{-1}·K^{-1} for H = 30 kOe) are comparable to our current work.

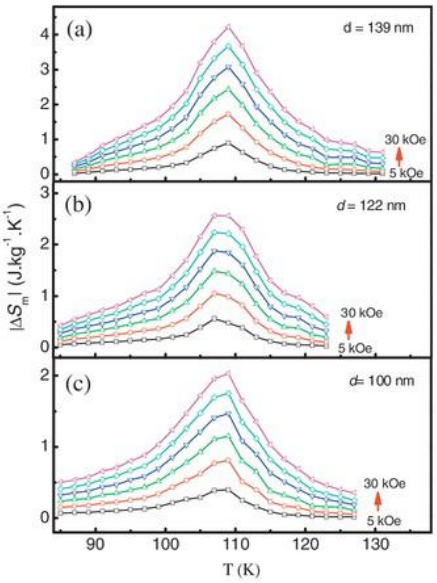

Fig. 4. $|\Delta S_m(T)|$ curves for the $Sm_{0.12}Ca_{0.88}MnO_3$ samples with (a) d = 139 nm, (b) d = 122 nm, and (c) d = 100 nm around the FM-PM phase transition in field intervals ranging from 5 to 30 kOe.

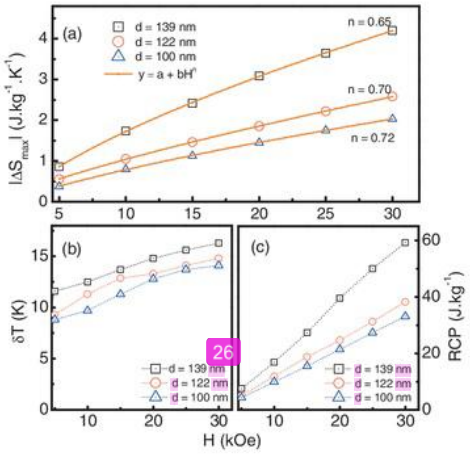

Fig. 5. (a) $|\Delta S_{max}(H)|$ data fitted to a power function of $|\Delta S_{max}| = a + b \cdot H^n$, (b) $\delta T(H)$ and (c) RCP(H) of the $Sm_{0.12}Ca_{0.88}MnO_3$ samples with d = 100–139 nm.

Together with magnetic-entropy change, the MC effect can also be assessed upon the refrigerative cooling power defined by RCP = $|\Delta S_{max}| \times \delta T$, where δT is the full-width-at-half maximum of a $|\Delta S_m(T)|$ curve, or upon the refrigerant capacity defined by $RC = -\int_{T_1}^{T_2} \Delta S_m(T) dT$, where T_1 and T_2 are the cold and hot ends of an ideal thermodynamic cycle [32]. Fig. 5(b, c) show temperature dependences of δT and RCP for the samples in the fields H ranging from 5 to 30 kOe. Similar to the variation tendency of $|\Delta S_{max}(H)|$, Fig. 5(a), both δT and RCP decrease gradually with decreasing d from 139 to 100 nm. For H = 30 kOe, RCP values are about 60, 38, and 33 J·kg^{-1} for d = 139, 122, and 100 nm, respectively. These values are about 10–20% higher than RC, depending on the magnitude of H.

The above assessments pointed out that all the samples have the SOPT nature, and FM order is declined with decreasing d from 139 nm to 100 nm. This influences directly the magnitude of M, $|\Delta S_{max}|$, and RCP (or RC). Recently, Franco et al. [32] suggested that if a single-phase magnetic material is measured at different T and H values, their $|\Delta S_m(T, H)|$ curves could be scaled into a universal curve. The scaling is carried out by normalizing $|\Delta S_m(T, H)|$ curves to their respective peak (ΔS_m^{pk}), $\Delta S\prime = |\Delta S_m(T,H)/\Delta S_m^{pk}$, with the temperature axis rescaled into $\theta = (T - T_C)/(T_r - T_C)$, where T_r is the reference temperature corresponding to a factor $f = \Delta S_m(T_r)/\Delta S_{max}$. The choice of f does not affect the construction of the universal curve. In Fig. 6, it shows the universal curves constructed for the d = 100–139 nm samples, where T_r values were selected to fulfill f = 0.5. The results in Fig. 6 reveal that almost $|\Delta S_m(T, H)|$ data points fall into a universal curve. This is in good agreement with the results shown in Refs. [32,35] and proves that our samples are magnetic single phase and undergo the SOPT. Concerning magnetic order, one can assess upon a magnetic-order parameter (N), which is calculated by using the following equation

$$N(T,H) = \frac{d \ln |\Delta S_m|}{d \ln H}. \quad (4)$$

For a ferromagnet undergoing the SOPT and exhibiting long-range magnetic interactions, N tends to 1, and is independent of H as $T \ll T_C$. It tends to 2 at temperatures $T \gg T_C$, and reaches a

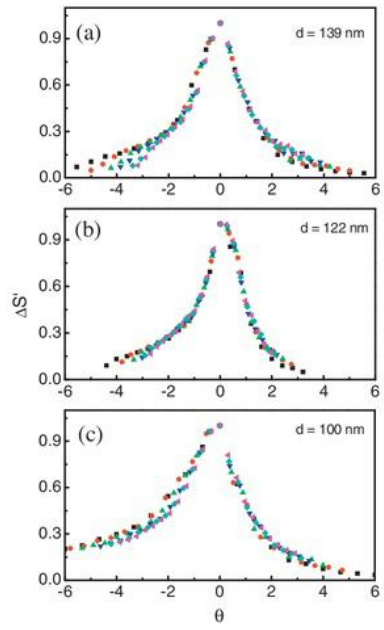

Fig. 6. Universal curves for the magnetic entropy of $Sm_{0.12}Ca_{0.88}MnO_3$ with (a) $d = 139$ nm, (b) $d = 122$ nm and (c) $d = 100$ nm in magnetic-field intervals ranging from 5 to 30 kOe.

minimum value equal to ~0.67 at $T = T_C$ [32]. The results shown in Fig. 7 reveal $N(T)$ values depend strongly on H. They tend to decrease and less changes as $H \geq 20$ kOe, because most magnetic moments were aligned to the H direction. The feature of the $N(T, H)$ curves also indicates the FM-PM transition separated by the minima around the T_C. Though the criteria for N in the $T \ll T_C$ and $T \gg T_C$ regions are fulfilled, its minimum (N_{min}) values of about 0.74, 0.76, and 0.79 for the $d = 139$, 122, and 100 nm samples, respectively (determined at the T_C for $H \geq 20$ kOe) are quite larger than the theoretical value of ~0.67. Similar to the variation tendency of n, N_{min} also increases with decreasing d to 100 nm,

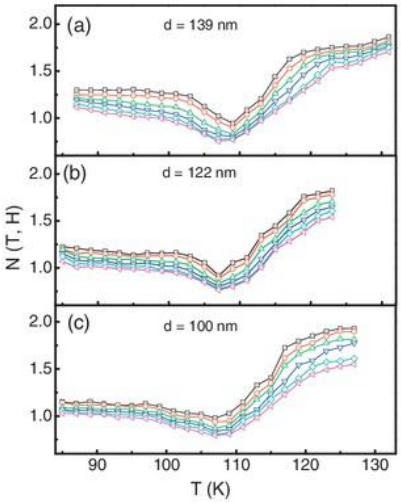

Fig. 7. $N(T, H)$ curves for $Sm_{0.12}Ca_{0.88}MnO_3$ samples with (a) $d = 139$ nm, (b) $d = 122$ nm and (c) $d = 100$ nm, where the field H varies in the range of 5–30 kOe.

indicating the decrease of long-range FM order. The difference between the N_{min} values and the theory value is related to the absence of perfect long-range magnetic interactions and the mixed phase of FM/AFM interactions in the samples with the existence of the Griffiths phase. With decreasing d to 100 nm, this phase would be widened.

4. Conclusion

We studied the magnetic and MC properties of the orthorhombic $Sm_{0.12}Ca_{0.88}MnO_3$ samples with $d = 100$–139 nm. The careful analyses of the $M(T, H)$ data based on the dM/dT versus T plots, Banerjee's criteria, and universal entropy curves (S') revealed all the samples exhibiting the SOPT nature, and undergoing the FM-PM phase transition at $T_C \approx 110$ K. The largest MC effect achieves around the corresponding the $|\Delta S_{max}|$ and RCP values to be about 2–4 $J \cdot kg^{-1} \cdot K^{-1}$, and 35–60 $J \cdot kg^{-1}$, respectively, for $H = 30$ kOe. Particularly, based on the analyses of the C-W law for the PM $\chi^{-1}(T)$ data, the feature of H/M versus M^2 curves, and the magnetic-order parameter $N(T, H)$, we found the samples having the existence of the Griffiths phase, and the transformation of long-range to short-range FM order when d decreases from 139 nm to 100 nm. This decrease of d leads to the formation of spin-glass-like surface layers, and reduces the FM correlation length, consequently the magnitude of M, $|\Delta S_{max}|$ and RCP (or RC) as recorded.

References

[1] J.S. Jung, A. Iyama, H. Nakamura, M. Mizumaki, N. Kawamura, Y. Wakabayashi, T. K[illegible]ra, Phys. Rev. B 82 (2010) 212403.
[2] V.Y. Ivanov, A.A. Mukhin, A.S. Prokhorov, A.M. Balbashov, Phys. Status Solidi B 236 (2003) 445.
[3] T. Kimura, S. Ishihara, H. Shintani, T. Arima, K.T. Takahashi, K. Ishizaka, Y. [illegible]ra, Phys. Rev. B 68 (2003) 060403(R).
[4] J.B. Goodenough, Localized to Itinerant Electronic Transition in Perovskite Oxides, Springer, New York, 2001.
[5] B. Kim, P. Tong, D. Kwon, Y. Wu, J.S. Ahn, I.K. Jeong, S.B. Kim, S.W. Cheong, B.G. [illegible] J. Appl. Phys. 105 (2009) 093927.
[6] M. Respaud, J.M. Broto, H. Rakoto, J. Vanacken, P. Wagner, C. Martin, A. Maignan, B. Raveau, Phys. Rev. B 63 (2001) 144426.
[7] [illegible]urbakov, A.V. Lazuta, V.A. Ryzhov, J. Phys.: Conf. Ser. 200 (2010) 012099.
[8] P. Lal, M.K. Dalai, R. Kundu, B.R. Sekhar, C. Martin, Phys. Rev. B 77 (2008) [illegible]05.
[9] Y. Tomioka, H. Hiraka, Y. Endoh, Y. Tokura, Phys. Rev. B 74 (2006) 104420.
[10] P. Tong, B. Kim, D. Kwon, T. Qian, S.I. Lee, S.W. Cheong, B.G. Kim, Phys. Rev. B 77 [illegible]8) 184432.
[11] M. Kasai, H. Kuwahara, Y. Tomioka, Y. Tokura, J. Appl. Phys. 80 (1996) 6894.
[12] N.S. Bingham, P.J. Lampen, T.L. Phan, M.H. Phan, S.C. Yu, H. Srikanth, J. Appl. Phys. 111 (2012) 07D[illegible].
[13] C. Zener, Phys. Rev. B 82 (1951) 403.
[14] A.J. Millis, P.B. Littlewood, B.I. Shraiman, Phys. Rev. Lett. 74 (1995) 5144.
[15] A.J. Millis, B.I. Shraiman, R. Mueller, Phys. Rev. Lett. 77 (1996) 175.
[16] C. Martin, A. Maignan, M. Hervieu, C. Autret, B. Raveau, D.I. Khomskii, Phys. [illegible] B 63 (2001) 174402.
[17] J. Hejtmanek, Z. Jirak, M. Marysko, C. Martin, A. Maignan, M. Hervieu, B. Raveau, Phys. Rev. B [illegible]999) 1457.
[18] A. Biswas, S. Chandra, M.H. Phan, H. Srikanth, J. Alloys Compd. 545 (2012) 157.
[19] R.S. Freitas, J. Ghivelder, F. Damay, F. Dias, L.F. Cohen, Phys. Rev. B 64 (2001) 144404.
[20] T.L. Phan, T.A. Ho, T.V. Manh, N.T. Dang, C.U. Jung, B.W. Lee, T.D. Thanh, J. Appl. [illegible]. 118 (2015) 143902.
[21] W. Jiang, X.Z. Zhou, G. Williams, Europhys. Lett. 84 (2008) 47009.
[22] S.M. Zhou, Y.Q. Guo, J.Y. Zhao, L.F. He, L. Shi, J. Phys. Chem. C 115 (5) (2011) 1535.
[23] [illegible] Baaziz, A. Tozri, E. Dhahri, E.K. Hlil, J. Magn. Magn. Mater. 403 (2016) 181.
[24] P. Lampen, N.S. Bingham, M.H. Phan, H. Kim, M. Osofsky, A. Pique, T.L. Phan, S. C. Y[illegible] Srikanth, Appl. Phys. Lett. 102 (2013) 062414.
[25] T.L. Phan, T.D. Thanh, P. Zhang, D.S. Yang, S.C. Yu, Solid State Commun. 166 [illegible]3) 32.
[26] L.E. Hueso, P. Sande, D.R. Miguéns, J. Rivas, F. Rivadulla, M.A. López-Quintela, J. [illegible] Appl. Phys. 91 (2002) 9943.
[27] A. [illegible]tt, J.E. Noakes, Phys. Rev. Lett. 19 (1967) 786.
[28] S.K. [illegible]nerjee, Phys. Lett. 12 (1964) 16.
[29] T.L. Phan, N.T. Dang, T.A. Ho, T.V. Manh, T.D. Thanh, C.U. Jung, B.W. Lee, A.T. Le, A.D. Phan, S.C. Yu, J. Alloys Compd. 657 (2015) 818.

[30] R. Skomski, Simple Models of Magnetism, Oxford University Press, New York, 2008.
[31] A.M. Tishin, Y.I. Spichkin, The Magnetocaloric Effect and its Applications, IOP Publishing Ltd, Bristol and Philadelphia, 2003.
[32] V. Franco, J.S. Blazquez, B. Ingale, A. Conde, Annu. Rev. Mater. Res. 42 (2012) 305.
[33] T.L. Phan, T.D. Thanh, T.A. Ho, T.V. Manh, Q.T. Tran, P. Lampen, M.H. Phan, S.C. Yu, I.E.E.E. Trans Magn. 50 (2014) 2302604.
[34] T.D. Thanh, D.C. Linh, N.T.U. Tuyen, T.L. Phan, S.C. Yu, J. Alloys Compd. 649 (2015) 981.
[35] C.M. Bonilla, J. Herrero-Albillos, F. Bartolomé, L.M. García, M. Parra-Borderías, V. Franco, Phys. Rev. B 81 (2010) 224424.

Magnetic and magnetocaloric properties of Sm1xCaxMnO3 (x = 0.88) nanoparticles

ORIGINALITY REPORT

19%	13%	17%	%
SIMILARITY INDEX	INTERNET SOURCES	PUBLICATIONS	STUDENT PAPERS

PRIMARY SOURCES

1	Min, S.G.. "Magnetocaloric properties of Gd"1"-"xB"x(x=0, 0.06, 0.09, 0.12) alloys", Journal of Magnetism and Magnetic Materials, 200608 Publication	1%
2	aist.hust.edu.vn Internet Source	1%
3	Aoyama, Takuya, Atsushi Miyake, Katsuya Shimizu, and Tsuyoshi Kimura. "Dielectric and AC-Calorimetry Measurements of SmMnO3 under High Pressure", Journal of the Physical Society of Japan, 2012. Publication	1%
4	etds.lib.ncku.edu.tw Internet Source	1%
5	Tran Dang Thanh, N. H. Dan, N. H. Duc, T. L. Phan, V. H. Ky, Jong Suk Lee, Seong-Cho Yu. "Ferromagnetic Order of Amorphous Fe-Ni-Zr Alloy Ribbons at Magnetic Field Below 10 kOe", Journal of Superconductivity and Novel	1%

Magnetism, 2016
Publication

6	S. M. Zhou, Y. Li, Y. Q. Guo, J. Y. Zhao, X. Cai, L. Shi. "Observation of a Griffiths-like phase in Ca-doped cobaltites", Journal of Applied Physics, 2013 Publication	<1%
7	Pękała, M., J. Szydłowska, K. Pękała, and V. Drozd. "Griffiths like phase in nanocrystalline manganite La0.50Ca0.50MnO3 studied by magnetic susceptibility and electron spin resonance", Journal of Alloys and Compounds, 2016. Publication	<1%
8	magneticmicrosphere.com Internet Source	<1%
9	glossparis.com Internet Source	<1%
10	N.N. Loshkareva, D.I. Gorbunov, A.V. Andreev, N.V. Mushnikov, Y. Skourski, F. Wolff-Fabris. "Metamagnetic transition of martensitic type in electron-doped manganites Ca1−xCexMnO3 (x=0.10, 0.12)", Journal of Alloys and Compounds, 2013 Publication	<1%
11	benasque.org Internet Source	<1%

12	Xie, Q.. "Evolution of A-site disorder-dependent structural and magnetic transport properties in La"2"/"3"-"xEu"xCa"1"/"3"-"ySr"yMnO"3", Materials Chemistry and Physics, 20090415 Publication	<1%
13	Xing Guo Gao, Bao Yuan Man, Mei Liu, Cheng Yang, Chuan Song Chen, Shou Zhen Jiang, Chun Ming Wang. "Impact of Nitrogen Pressure on the Structural, Morphologic and Magnetic Properties of the GaMnN Thin Films", Journal of Superconductivity and Novel Magnetism, 2013 Publication	<1%
14	Iyama, Ayato, Jong-Suck Jung, Eun Sang Choi, Jungmin Hwang, and Tsuyoshi Kimura. "High-Magnetic-Field Effect on Interplay between Sm 4f and Mn 3d Moments in SmMnO3", Journal of the Physical Society of Japan, 2012. Publication	<1%
15	Nguyen, Duy-Cuong, Seigo Ito, and Dang Viet Anh Dung. "Effects of annealing conditions on crystallization of the CZTS absorber and photovoltaic properties of Cu(Zn,Sn)(S,Se)2 solar cells", Journal of Alloys and Compounds, 2015. Publication	<1%
16	Abdelkhalek, S.B.. "Transport behavior and	

	mechanism of conduction of simultaneously substituted Y and Fe in La"0"."7Ba"0"."3MnO"3 perovskite", Physica B: Physics of Condensed Matter, 20111101 Publication	<1%
17	Skini, R., M. Khlifi, and E. K. Hlil. "An efficient composite magnetocaloric material with a tunable temperature transition in K-deficient manganites", RSC Advances, 2016. Publication	<1%
18	Tran Dang Thanh, Le Viet Bau, T. L. Phan, S. C. Yu. "Room Temperature Magnetocaloric Effect in ${\hbox{La}}_{0.7}{\hbox{Sr}}_{0.3}{\hbox{Mn}}_{1\hbox{-}{\rm x}}{\hbox{Co}}_{\rm x}{\hbox{O}}_{3}$", IEEE Transactions on Magnetics, 2014 Publication	<1%
19	Chan-Chieh Lin, R. Lydia, Jae Hyun Yun, Ho Seong Lee, Jong Soo Rhyee. " Extremely Low Lattice Thermal Conductivity and Point Defect Scattering of Phonons in Ag-doped (SnSe) (SnS) Compounds ", Chemistry of Materials, 2017 Publication	<1%
20	dspace.lboro.ac.uk Internet Source	<1%
21	Petr, T.. "On the physical properties of Sr"1"-	

	"xNa"xRuO"3 (x=0-0.19)", Solid State Sciences, 201007 Publication	<1%
22	V. Markovich. "Effect of pressure on magnetic and transport properties of CaMn_{1−x}Ru_{x}O_{3} (x=0–0.15): Collapse of ferromagnetic phase in CaMn_{0.9}Ru_{0.1}O_{3}", Physical Review B, 07/2004 Publication	<1%
23	pastel.archives-ouvertes.fr Internet Source	<1%
24	A. Arabi, M. Fazli, M.H. Ehsani. "Tuning the morphology and photocatalytic activity of La0.7Ca0.3MnO3 nanorods via different mineralizer-assisted hydrothermal syntheses", Materials Research Bulletin, 2017 Publication	<1%
25	www.dtic.mil Internet Source	<1%
26	Y.G. Li, S.F. Mao, Z.J. Ding. "Chapter 11 Monte Carlo Simulation of SEM and SAM Images", InTech, 2011 Publication	<1%
27	www.acrhem.org Internet Source	<1%

28	Yang, Yang, Yikun Zhang, Xiao Xu, Shuhua Geng, Long Hou, Xi Li, Zhongming Ren, and Gerhard Wilde. "Magnetic and magnetocaloric properties of the ternary cadmium based intermetallic compounds of Gd2Cu2Cd and Er2Cu2Cd", Journal of Alloys and Compounds, 2016. Publication	<1%
29	www.nplindia.org Internet Source	<1%
30	Bousquet, Eric, and Andrés Cano. "Non-collinear magnetism in multiferroic perovskites", Journal of Physics Condensed Matter, 2016. Publication	<1%
31	www.vlab.msi.umn.edu Internet Source	<1%
32	www.mysciencework.com Internet Source	<1%
33	Ogimoto, Y.. "The essentials for the control of charge-orbital ordering in thin films of perovskite manganites", Materials Science & Engineering B, 20101015 Publication	<1%
34	researchpub.org Internet Source	<1%

35	www.tandfonline.com Internet Source	<1%
36	"Table of contents", IEEE Transactions on Magnetics, 2015. Publication	<1%
37	Hcini, S.. "Critical phenomena in Pr"0"."6Sr"0"."4MnO"3 perovskite manganese oxide", Solid State Sciences, 201205 Publication	<1%
38	N. Adeela, U. Khan, S. Naz, M. Iqbal, M. Irfan, Y. Cheng. "Low temperature nucleation of Griffiths Phase in Co doped LaMnO3 nanostructures", Applied Surface Science, 2017 Publication	<1%
39	Kameli, P.. "Influence of grain size on magnetic and transport properties of polycrystalline La"0"."8Sr"0"."2MnO"3 manganites", Journal of Alloys and Compounds, 20080214 Publication	<1%
40	www.qucosa.de Internet Source	<1%
41	www.fs.fed.us Internet Source	<1%
42	DENG, J.. "Effect of gallium doping on the magnetocaloric effect of	<1%

LaFe"1"1"."2Co"0"."7Si"1"."1", Rare Metals, 200808
Publication

---

43 Luo, X.. "Complex ferromagnetic state transformation in single crystal Nd"0"."5Pb"0"."5MnO"3", Journal of Magnetism and Magnetic Materials, 201002 <1%
Publication

---

44 Phan, T.L.. "Spin dynamics in annealed Mn-doped ZnO ceramic materials", Solid State Communications, 200710 <1%
Publication

---

45 P. Sarkar. "Large magnetocaloric effect in Sm[sub 0.52]Sr[sub 0.48]MnO[sub 3] in low magnetic field", Applied Physics Letters, 2008 <1%
Publication

---

46 A Ben Jazia Kharrat, E K Hlil, W Boujelben. "Prediction of magnetic and magnetocaloric properties in $$\hbox {Pr}_{0.8-x}\hbox {Bi}_{x}\hbox {Sr}_{0.2}\hbox {MnO}_{3}$$ Pr 0.8 - x Bi x Sr 0.2 MnO 3 ($$x=0$$ x = 0 , 0.05 and 0.1) manganites", Bulletin of Materials Science, 2019 <1%
Publication

---

47 www.revistacubanadefisica.org <1%
Internet Source

---

oacis.repo.nii.ac.jp

48	Internet Source	<1%
49	depositonce.tu-berlin.de Internet Source	<1%
50	Z. C. Xia. "Magnetic phase boundary and transport properties of La0.67Ca0.33MnO3", physica status solidi (b), 07/2005 Publication	<1%
51	ddl.escience.cn Internet Source	<1%
52	www.osti.gov Internet Source	<1%
53	Biswas, Anis, Sayan Chandra, Manh-Huong Phan, and Hariharan Srikanth. "Magnetocaloric properties of nanocrystalline LaMnO3: Enhancement of refrigerant capacity and relative cooling power", Journal of Alloys and Compounds, 2012. Publication	<1%
54	Gusmao, M.A.. "Disorder effects at low temperatures in La"0"."7"-"xY"xCa"0"."3MnO"3 manganites", Solid State Communications, 200309 Publication	<1%
55	pdfs.semanticscholar.org Internet Source	<1%

56	Bellouz, R., M. Oumezzine, E.K. Hlil, and E. Dhahri. "Critical behavior near the ferromagnetic–paramagnetic phase transition in La0.65Eu0.05Sr0.3Mn1−xCrxO3 (x=0.10 and x=0.15)", Physica B Condensed Matter, 2015. Publication	<1%
57	C. M. Xiong. "Structure, magnetic, and transport properties of the perovskites Bi[sub 0.5]Ca[sub 0.5]Mn[sub 1−x]Cr[sub x]O[sub 3]", Journal of Applied Physics, 2004 Publication	<1%
58	Abassi, Mounira, N. Dhahri, J. Dhahri, and E.K. HLIL. "Structural and large magnetocaloric properties of La0.67−xYxBa0.23Ca0.1MnO3 perovskites (0≤x≤0.15)", Physica B Condensed Matter, 2014. Publication	<1%
59	Mañosa, Lluís, Antoni Planes, and Mehmet Acet. "Advanced materials for solid-state refrigeration", Journal of Materials Chemistry A, 2013. Publication	<1%
60	N. N. Loshkareva. "Charge ordering melting in CaMnO_{3−δ} single crystals with ordered oxygen vacancies", Physical Review B, 02/2008 Publication	<1%
	Pramod Kumar. "Magnetic, magnetothermal,	

61	and magnetotransport properties in SmMn[sub 2]Si[sub 2−x]Ge[sub x] compounds", Journal of Applied Physics, 2008 Publication	<1%
62	www.conicet.gov.ar Internet Source	<1%
63	B. C. Zhao. "Magnetic and magnetocaloric properties of Cu-substituted La[sub 1−x]Pb[sub x]MnO[sub 3] (x∼0.14) single crystals", Journal of Applied Physics, 2007 Publication	<1%
64	Chau, N.. "The discovery of the colossal magnetocaloric effect in a series of amorphous ribbons based on Finemet", Materials Science & Engineering A, 20070325 Publication	<1%
65	www.nbro.gov.lk Internet Source	<1%
66	asl.korea.ac.kr Internet Source	<1%
67	Anita Semwal. "Low-lying magnetic excitations in Ni_{3}Al and their suppression by a magnetic field", Physical Review B, 11/1999 Publication	<1%
68	Hazzez, M., N. Ihzaz, M. Boudard, and M. Oumezzine. "Crystal structure, phase	<1%

transitions, and magnetic properties of titanium doped La0.5Sr0.5MnO3 perovskites", Physica B Condensed Matter, 2016.

Publication

Exclude quotes	Off	Exclude matches	Off
Exclude bibliography	Off		